SCATTERING FROM A CORRUGATED THICK SCREEN

M. Albani[1], *F. Capolino*[2], *P. Piazzesi*[1], *S. Maci*[2], *R. Tiberio*[1]

[1]*College of Engineering, Univ. of Siena, Via Roma 56, Siena, Italy*
[2]*Dept. of Elec. Eng., Univ. of Florence, Via S.Marta 3, Florence, Italy*

1. INTRODUCTION

A closed form, high-frequency solution is presented for the scattering in the near zone by a semi-infinite thick screen, when it is illuminated by a line source at finite distance. This solution is derived for a thick screen with perfectly conducting side walls, and either perfectly conducting or artificially soft boundary condition [1] on the top face joining the two wedges. This last condition is practically obtained by etching on this face a quarter of wavelength deep corrugations with a small periodicity with respect to the wavelength. Owing to the particular properties of the artificially soft surface, a strong decoupling effect in the shadow region is achieved for both polarizations; thus, an effective shielding from undesired interferences is obtained.

The formulation adopted in this paper, which is based on the spectral approach presented in [2],[3], is briefly summarized in Sect. 2. The artificially soft boundary condition is accounted for by the spectral Green's function derived in [4],[5]. The above procedure leads to a double spectral integral that is asymptotically evaluated in Sect. 3. Thus, a high-frequency solution is obtained, that is described as a superposition of different diffracted field contributions, including doubly diffracted rays. This solution uniformly describes the total field, including those aspects where the transition regions of the diffracted fields from the two edges overlap, and an ordinary application of standard UTD [6] fails. Numerical results are presented and discussed in Sect. 4 in order to emphasize the shielding effectiveness of the corrugated screen.

2. FORMULATION

The geometry of the problem is shown in Fig. 1. Let us define a cylindrical coordinate system (ρ_i, ϕ_i) [1] at each edge $i = 1,2$. A uniform either electric (TM_z) or magnetic (TE_z) line source illumination is assumed. Also, let us denote by $P' \equiv (\rho_1', \phi_1')$ the source point and by ℓ the thickness of the screen. The incident field at any point $P \equiv (\rho_1, \phi_1)$ is either

$$E_z = -jk\zeta I_e \psi(P,P') \quad \text{or} \quad H_z = -j\frac{k}{\zeta} I_m \psi(P,P') \tag{1}$$

for either TM_z or TE_z case, respectively, where

$$\psi(P,P') = \frac{1}{4j} H_0^{(2)}(k|P-P'|), \tag{2}$$

and I_e, I_m are the amplitudes of the electric and magnetic currents.

For the sake of simplicity in the notation we deal with the normalized scalar potential ψ.

The total field is represented as the sum of the GO field plus singly diffracted fields from edges 1 and 2, and doubly diffracted fields. In order to calculate the doubly diffracted contribution, the same formulation as that used in [2],[3] is used, which is summarized hereinafter. First, the response of the first edge to the line source excitation is represented in terms of a cylindrical wave spectrum. Next, each cylindrical spectral source is used as the incident field at the second edge. Then, the near field response of the second wedge is employed to obtain, by spectral synthesis, a double integral representation of the doubly diffracted field

$$\psi_{12}^{dd} = -\frac{1}{4\pi^2}\sum_{p,q=1}^{2}(-1)^{p+q}\int_{-j\infty}^{j\infty}\int_{-j\infty}^{j\infty}\frac{1}{4j}H_0^{(2)}(kR(\alpha_1,\alpha_2))\cdot \\ \cdot F_1(\Phi_1^p,\alpha_1)\,F_2(\Phi_2^q,\alpha_2)\,d\alpha_1\,d\alpha_2 \tag{3}$$

in which

$$R(\alpha_1,\alpha_2) = \sqrt{\rho_1'^2+\ell^2+\rho_2{}^2+2\rho_1'\ell\,\cos\alpha_1+2\rho_2\ell\,\cos\alpha_2+2\rho_1'\rho_2\cos(\alpha_1+\alpha_2)}. \tag{4}$$

In (3), the spectral functions F_i have different expressions for the the different cases that are shown in Fig. 1 [4],[5]; i.e.,

$$F_i(\Phi,\alpha) = \frac{1}{n_i}\frac{f_i^{h,a,s}(\Phi,\alpha)}{\cos\frac{\alpha}{n_i}-\cos\frac{\Phi}{n_i}} \tag{5}$$

in which

$$f_i^h(\Phi,\alpha) = \sin\frac{\Phi}{n_i};\quad f_i^a(\Phi,\alpha)=2\cos\frac{\Phi}{2n_i}\sin\frac{\alpha}{2n_i};\quad f_i^s(\Phi,\alpha)=\sin\frac{\alpha}{n_i}; \tag{6}$$

where superscripts h, a denote the TE_z polarization for hard (Fig 1a), artificially soft (Fig. 1b), respectively, and s the TM_z polarization for both configurations. Furthermore, $\Phi_1^p=\phi_1'+(-1)^p\pi$; $\Phi_2^q=\phi_2+(-1)^q\pi$. It is rather apparent that expression (8) explicitly satisfies reciprocity.

An anolougus double diffraction contribution ψ_{21}^{dd} arises from the reverse mechanism 2→1.

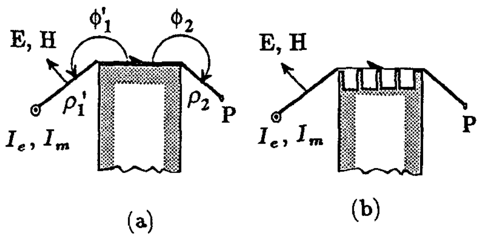

Fig. 1 *Geometry of the problem*

3. HIGH-FREQUENCY SOLUTION.

The double spectral integral representation for ψ_{12}^{dd} is now asymptotically evaluated to find a uniform high-frequency expression. To this end, it is seen that the integrand in (8) exhibits a two dimensional, stationary phase point at $(\alpha_1,\alpha_2) = (0,0)$, that provides the dominant contribution. Furthermore, $F_1(\Phi_1^p, \alpha_1)$ and $F_2(\Phi_2^q, \alpha_2)$ exhibit pole singularities that independently occur in the two spectral variables. These poles may occur close to and at the stationary point; thus, they have to be appropriately accounted for. The uniform asymptotic evaluation of ψ_{12}^{dd} is performed by considering the nearest poles to the saddle point. It is worth noting that the functions F_i are either even or odd with respect to the integration variable for either hard (h) or artificially soft (a) and soft (s) cases. In these latter cases, the integrand vanish at the saddle point; thus, requiring a more accurate asymptotic evaluation, as that in [3]. This leads to

$$\psi_{12}^{dd} \sim \frac{1}{2\sqrt{2\pi jk}} \frac{e^{-jk(\rho_1' + \ell + \rho_2)}}{\sqrt{\rho_1'\ell\rho_2}} \; D_{12}^{h,a} \tag{7}$$

where $D_{12}^{h,a,s}$ are the double diffraction coefficients for hard (h), artificially soft (a) and soft (s) cases, that are expressed as

$$D_{12}^{h} = \frac{1}{4\pi jk} \cdot \sum_{p,q=1}^{2} \frac{(-1)^{p+q}}{n_1 n_2} \cot\left(\frac{\Phi_1^p}{2n_1}\right) \cot\left(\frac{\Phi_2^q}{2n_2}\right) \cdot \widetilde{T}(a_p, b_q, w) \ ,$$

$$D_{12}^{a} = \frac{-1}{4\pi^2 k^2 \ell} \cdot \sum_{p,q=1}^{2} \frac{(-1)^{p+q}}{(n_1 n_2)^2} \frac{\cos\left(\frac{\Phi_1^p}{2n_1}\right)}{\sin^2\left(\frac{\Phi_1^q}{2n_1}\right)} \frac{\cos\left(\frac{\Phi_2^q}{2n_2}\right)}{\sin^2\left(\frac{\Phi_2^q}{2n_2}\right)} \cdot \widetilde{\widetilde{T}}(a_p, b_q, w) \ , \tag{8}$$

and

$$D_{12}^{s} = \frac{-1}{4\pi^2 k^2 \ell} \cdot \sum_{p,q=1}^{2} \frac{(-1)^{p+q}}{(n_1 n_2)^2} \csc^2\left(\frac{\Phi_1^p}{2n_1}\right) \csc^2\left(\frac{\Phi_2^q}{2n_2}\right) \cdot \widetilde{\widetilde{T}}(a_p, b_q, w).$$

Expressions (8) involve the transition functions

$$\widetilde{T}(a,b,w) = \frac{2\pi jab}{\sqrt{1-w^2}} \left[\mathcal{G}(a,\frac{wa+b}{\sqrt{1-w^2}}) + \mathcal{G}(b,\frac{wb+a}{\sqrt{1-w^2}}) + \mathcal{G}(a,\frac{wa-b}{\sqrt{1-w^2}}) + \mathcal{G}(b,\frac{wb-a}{\sqrt{1-w^2}}) \right]$$

and (9)

$$\widetilde{\widetilde{T}}(a,b,w) = \frac{-4\pi(ab)^2}{w\sqrt{1-w^2}} \left[\mathcal{G}(a,\frac{wa+b}{\sqrt{1-w^2}}) + \mathcal{G}(b,\frac{wb+a}{\sqrt{1-w^2}}) - \mathcal{G}(a,\frac{wa-b}{\sqrt{1-w^2}}) - \mathcal{G}(b,\frac{wb-a}{\sqrt{1-w^2}}) \right]$$

in which $\mathcal{G}$ is the Generalized Fresnel Integral defined as in [7] where a very simple algorithm is suggested for its numerical computation. The distance parameters involved in the transition functions are:

$$a_p = \sqrt{2k\frac{\rho_1'\ell}{\rho_1'+\ell}} \sin\left(\frac{\Phi_1^p - 2n_1 N^p \pi}{2}\right), \quad b_q = \sqrt{2k\frac{\rho_2\ell}{\rho_2+\ell}} \sin\left(\frac{\Phi_2^q - 2n_2 N^q \pi}{2}\right) \tag{10}$$

where N^p, N^q are integers defined as in the standard UTD [6], and

$$w = \sqrt{\frac{\rho_1^i \rho_2}{(\rho_1^i + \ell)(\ell + \rho_2)}} \ . \tag{11}$$

4. NUMERICAL EXAMPLES

Several numerical results have been calculated. One example is shown in Fig. 2 which refers to a thickness $\ell = \lambda/4$. There, the total field is plotted when the observation point moves from the lit to shadowed face as depicted in the inset. It is seen that in the soft and artificially soft cases the field in the shadow region is much weaker than that in the hard case. This emphasizes that the corrugations on the top face provides a strong shielding effect even for TE_z polarization. Indeed even for such a small thickness the shielding effect in the shadow region for the TE_z case is improved by about 10 dB. Increasing the thickness of the corrugated face dramatically increases the shielding in the shadow region.

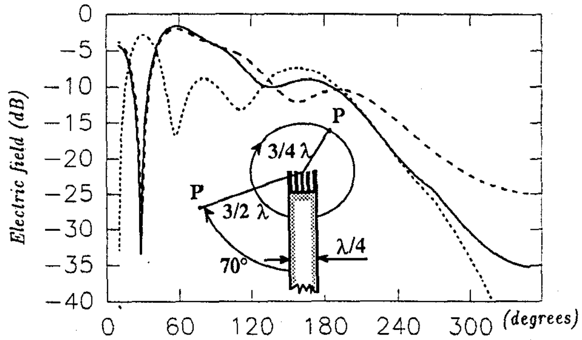

Fig. 2 *Electric field amplitude. TE_z, perfectly conducting (dashed line); TE_z, artificially soft (solid line); TM_z, (dotted line)*

References

[1] P-S. Kildal, "Artificially soft and hard surfaces in electromagnetics," *IEEE Trans. Antennas Propagat.*, vol. AP-38, pp. 1537-1544, Oct. 1990.

[2] M. Albani, F. Capolino, S. Maci, R. Tiberio, "Double Diffraction Coefficients for Source and Observation at Finite Distance for a Pair of Wedges", *IEEE AP-S Symposium,* NewPort Beach, June 18-23, 1995.

[3] F. Capolino, M. Albani, S. Maci, R. Tiberio,"Diffraction From a Couple of Coplanar, Skew Wedges", *Submitted to IEEE Trans. on Ant. Propagat.*

[4] S. Maci, R. Tiberio, A. Toccafondi,"Diffraction Coefficients at Edges in artificially Soft and Hard Surfaces", *Electr. Letters*, V.30, N.3, Febr. 1994.

[5] M. Leoncini, S. Maci, A. Toccafondi, "Analysis of the Electromagnetic Scattering by Artificially Soft Discs" *IEE proc. H,* vol 142, n. 5, pp. 399-404 , Oct. 1995

[6] R. G. Kouyoumjian and P. H. Pathak, "A uniform geometrical theory of diffraction for an edge in a perfectly conducting surface," *Proc. IEEE*, vol. 62, n.11, pp. 1448-1461, Nov. 1974.

[7] F. Capolino, S. Maci, "Simplified Closed-Form Expressions for Computing the Generalized Fresnel Integral and Their Application to Vertex Diffraction", *Microw. Opt. Techn. Letters,* V.9, N.1, May 1995.